

COMPONENT PART NOTICE

THIS PAPER IS A COMPONENT PART OF THE FOLLOWING COMPILATION REPORT:

TITLE: Proceedings of the U.S. Air Force and the Federal Republic of Germany Data Exchange Agreement Meeting (9th), Viscous and Interacting Flow Field Effects Held at Silver Spring, Maryland on 9-10 May 1984.

TO ORDER THE COMPLETE COMPILATION REPORT, USE AD-A153 020.

THE COMPONENT PART IS PROVIDED HERE TO ALLOW USERS ACCESS TO INDIVIDUALLY AUTHORED SECTIONS OF PROCEEDING, ANNALS, SYMPOSIA, ETC. HOWEVER, THE COMPONENT SHOULD BE CONSIDERED WITHIN THE CONTEXT OF THE OVERALL COMPILATION REPORT AND NOT AS A STAND-ALONE TECHNICAL REPORT.

THE FOLLOWING COMPONENT PART NUMBERS COMPRISE THE COMPILATION REPORT:

AD#: POOL 787 - AD-POOL 800 AD#: _____
 AD#: _____ AD#: _____
 AD#: _____ AD#: _____

S DTIC ELECTE **D**
 JUL 23 1985
B

Accession For	
NTIS GRA&I	<input checked="" type="checkbox"/>
DTIC TAB	<input type="checkbox"/>
Unannounced	<input type="checkbox"/>
Justification	
By _____	
Distribution/	
Availability Codes	
Dist	Avail and/or Special
A-1	

DISTRIBUTION STATEMENT A
 Approved for public release
 Distribution Unlimited

AD-P004 787

A Discrete Element Prediction Approach for
Turbulent Flow Over Rough Surfaces

by

Robert P. Taylor, Hugh W. Coleman and B. Keith Hodge
Mechanical and Nuclear Engineering Department
Mississippi State University
Mississippi State, MS 39762

ABSTRACT

A discrete element model for turbulent flow over rough surfaces has been rigorously derived from basic principles. This model includes surface roughness effects as a constituent part of the partial differential equations which describe momentum and energy transport in turbulent flows. The model includes the necessary empirical information on the interaction between the roughness elements and the flow around and between the elements in a general way which does not require experimental data on each specific surface. This empirical information is input via algebraic models for the local element drag coefficient and Nusselt number. These models were calibrated by comparison with base data sets from surfaces with three-dimensional (distributed) roughness elements. Calculations using the present model have been compared with experimental data from 118 separate experimental runs. The results of these comparisons ranged from good to excellent. The calculations compared equally well with both transitionally rough and fully rough turbulent flow results without modification of the roughness model.

1. Introduction

In this paper, the authors present a synopsis of the results of a research effort on the prediction of skin friction and heat transfer in turbulent flow over rough surfaces. Details of the development of the discrete element approach, a review of previous work, and more comparisons of predictions with experimental data can be found in References 1-3.

2. Modeling of Roughness Effects on Turbulent Flow

In turbulent flow analysis, use of time-averaged equations leads to the necessity of formulating a turbulence model (with empirical input) to achieve closure. A similar situation exists in analysis of flow over rough surfaces. Unless the equations can be solved on a grid which is fine enough to resolve the surface roughness boundary condition, a roughness model (with empirical input) is necessary for closure. Considering the capabilities of present computers, both turbulence and roughness models must be formulated for analysis of practical problems in turbulent flow over rough surfaces. In References 1-3, the authors have described in detail both the classical equivalent sandgrain roughness approach and their discrete element method which incorporates more basic physics of the surface-flow interaction and requires less surface-specific empirical information. A summary is presented below.

Schlichting (4) first proposed the equivalent sandgrain roughness (k_s) concept and experimentally determined k_s for a range of rough surfaces. He defined k_s as the size of sandgrain in Nikuradse's (5) pipe flow experiments which would give the same skin friction as that observed on a particular rough surface. One problem in using this approach is determining k_s for a specific surface of interest when no skin friction data are available for that surface. Dvorak (6), Simpson (7) and Dirling (8) all presented correlations which essentially allowed k_s to be determined based on various geometric characteristics of the roughness elements on the surface. These correlations suffer from two basic problems: (1) they do not correlate the available data well, and (2) they rely primarily on Schlichting's experimental results. The authors (9) have shown that, due to erroneous assumptions in data reduction, Schlichting's results for skin friction are high by amounts

ranging up to 73% and his results for k_s are high by 26% to 555%. Thus the validity of previous roughness work which has relied heavily on Schlichting's results is open to serious question. In addition, the idea that the effects of all rough surfaces can be modeled using a single length scale (k_s) has not been successful in application.

The discrete element roughness model of the authors is totally divorced from any k_s concepts. In formulating the model, the continuity, momentum and energy equations for a boundary layer were derived from first principles. Included in the derivations were the influences of the surface roughness elements which are shown in Figure 1. These influences are the blockage, the form drag, and the local heat transfer between the fluid and the elements.

The resulting equations, formulated for the special case of three-dimensional uniform roughness elements (such as spheres, hemispheres, cones, etc.), are shown in Figure 2. The shape, size and spacing of the elements are included explicitly through the geometrical descriptors of the roughness-- $D(y)$, L and ℓ . The empirical information is input through algebraic expressions for the element drag coefficient

$$C_D = C_D(\text{Re}(y))$$

and element Nusselt number

$$\text{Nu} = \text{Nu}(\text{Re}(y)) \quad .$$

The C_D model was calibrated using the corrected (9) skin friction data sets of Schlichting (4) for surfaces with roughness elements of spherical, spherical segment, and conical shapes. The Nu model was calibrated using a zero pressure gradient, constant wall temperature data set of Pimenta (10) for a surface of spherical elements in the most dense packing. Once the C_D and Nu models were calibrated, they remained invariant for all subsequent calculations. No empirical information is used for any specific rough surface--only the geometrical description of the roughness is input for "new" surfaces with three-dimensional type roughness. Comparisons of calculations with the calibration data are shown in Figures 3-6.

3. Comparisons of Predictions and Data

Comparisons of discrete element model predictions with various additional data sets are presented in References 1-3. Comparisons of predictions with the data of two experimental investigations are presented here as an indication of the merit of the discrete element model.

Chen (11) reported detailed turbulence and skin friction measurements for fully developed air flow through a 0.19 meter diameter pipe roughened with hemispheres. He investigated three roughness densities-- $\ell/k = 18.5$, 10.7 and 6.4, where k is the maximum roughness element height. Chen stated that the first two cases ($\ell/k = 18.5$ and 10.7) were in the transitionally rough regime and the third ($\ell/k = 6.4$) was "nearly" in the fully rough regime. The most interesting part of Chen's work (from the point of view of the present work) is the segregation of the two components of the apparent wall shear stress: (1) that due to the viscous shear (τ_s) on the smooth surface between the roughness elements, and (2) that due to the form drag on the roughness elements. Chen obtained the form drag term by measuring the force on a single element using a force balance. The portion due to the smooth surface was determined by subtracting the roughness element drag component from the total wall shear stress (τ_T) which was determined from pressure drop measurements.

The discrete element model was solved in the appropriate internal circular coordinates and the resulting predictions were compared with Chen's data. Figure 7 shows the comparisons for the skin friction coefficient and the ratio of the smooth wall component to the total shear stress. The comparisons indicate very good agreement. The comparisons of the relative contribution of viscous shear forces between the elements and the drag on the elements are of particular interest. One of the major advantages of the discrete element model is that these two forces and their interactions are accounted for in the model. Inspection of Figure 7 reveals good agreement between the predictions and data for τ_s/τ_T . The maximum disagreement is about 12% and the preponderance of the points agree within 5%. This agreement indicates that the present discrete element model correctly incorporates much of the physics of the interaction between the roughness elements and the flow.

Coleman (12) reported turbulence measurements and skin friction and Stanton number measurements for turbulent boundary layer air flows

over a flat plate with 1.27 mm diameter spherical roughness elements in the most dense packing. Shown in Figure 8 are comparisons of the discrete element model predictions with data for a constant wall temperature, favorable pressure gradient case. The boundary layer was in the fully rough flow regime. The agreement is excellent, with the predictions everywhere within the data uncertainty. Shown in Figure 9 are comparisons of the predictions with data for a variable wall temperature, zero pressure gradient case. Again, the agreement is excellent.

4. Summary

Several points which should be emphasized are: (1) NO information from the Chen or Coleman data sets other than the geometrical description of the rough surfaces was used in the discrete element model calculations. The calculations are therefore truly predictions. (2) The turbulence model used was the standard mixing length model with Van Driest damping, which is widely used for smooth wall flows. No modifications were made because of the roughness. (3) The present discrete element model has been formulated and proven only for three-dimensional type roughness elements which can be approximated as having circular cross-sections in the xz plane. (The development for such elements which are randomly shaped and are of random spacing is given in References 1-3).

This research was sponsored by the Air Force Armament Laboratory, Eglin Air Force Base, FL. under contract F08635-82-K-0062. The authors wish to thank Lt Bruce Haupt, Dr. Lawrence Lijewski and Dr. Donald Daniel for their support and encouragement.

REFERENCES

1. Coleman, H. W., Hodge, B. K., and Taylor, R. P., "Generalized Roughness Effects on Turbulent Boundary Layer Heat Transfer," USAF AFATL-TR-83-90, November 1983.
2. Taylor, R. P., Coleman, H. W., and Hodge, B. K., "A Discrete Element Prediction Approach for Turbulent Flow Over Rough Surfaces," Report TFD-84-1, Mech. and Nuc. Eng. Dept., Miss. State Univ., February 1984.
3. Taylor, R. P., "A Discrete Element Prediction Approach for Turbulent Flow Over Rough Surfaces," Ph.D. Dissertation, Mississippi State University, 1983.
4. Schlichting, H., "Experimental Investigation of the Problem of Surface Roughness," Ingenieur-Archiv, Vol. VII, No. 1, 1936; NACA TM 823, 1937.
5. Nikuradse, J., "Laws for Flows in Rough Pipes," VDI-Forschungsheft 361, Series B, Vol. 4, 1933; NACA TM 1292, 1950.
6. Dvorak, F. A., "Calculation of Turbulent Boundary Layers on Rough Surfaces in Pressure Gradients," AIAA Journal, Vol. 7, 1969, pp. 1752-1759.
7. Simpson, R. L., "A Generalized Correlation of Roughness Density Effects on the Turbulent Boundary Layer," AIAA Journal, Vol. 11, 1973, pp. 242-244.
8. Dirling, R. B., Jr., "A Method for Computing Rough Wall Heat Transfer Rates on Reentry Nose Tips," AIAA Paper No. 73-763, 1973.
9. Coleman, H. W., Hodge, B. K., and Taylor, R. P., "A Re-Evaluation of Schlichting's Surface Roughness Experiment," accepted for publication in J. Fluids Engrg., 1984.
10. Pimenta, M. M., "The Turbulent Boundary Layer: An Experimental Study of the Transport of Momentum and Heat with the Effect of Roughness," Ph.D. Dissertation, Dept. Mech. Eng., Stanford Univ., 1975; Report HMT-21.
11. Chen, C. K., "Characteristics of Turbulent Flow Resistance in Pipes Roughened with Hemispheres," Ph.D. Dissertation, Washington State Univ., 1971.
12. Coleman, H. W., "Momentum and Energy Transport in the Accelerated Fully Rough Turbulent Boundary Layer," Ph.D. Dissertation, Dept. Mech. Eng., Stanford Univ., 1976; Report HMT-24.

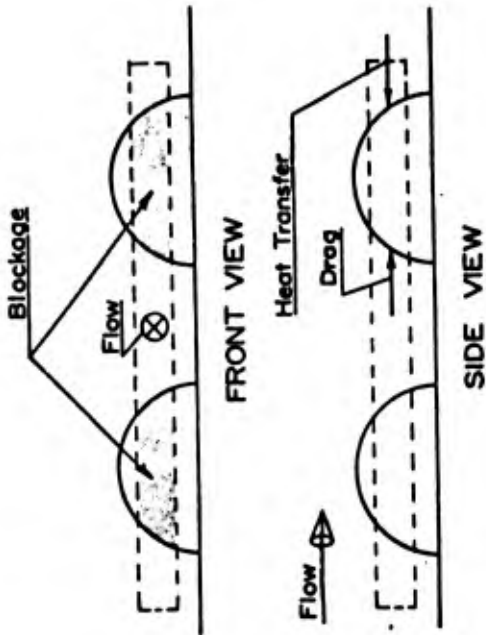


Figure 1. Schematic of Rough Surface Showing Physical Effects Included in Discrete Element Modeling Approach

MASS:

$$\frac{\partial}{\partial x} (\rho \beta_{yz} u) + \frac{\partial}{\partial y} (\rho \beta_{xz} v) = 0$$

MOMENTUM:

$$\rho \beta_{yz} u \frac{\partial u}{\partial x} + \rho \beta_{xz} v \frac{\partial u}{\partial y} = - \frac{\partial}{\partial x} (\beta_{yz} P) + \frac{\partial}{\partial y} (\beta_{xz} \tau) - \rho C_D u^2 D(y) / 2Lx$$

ENERGY:

$$\rho \beta_{yz} u \frac{\partial h}{\partial x} + \rho \beta_{xz} v \frac{\partial h}{\partial y} = - \frac{\partial}{\partial y} (\beta_{xz} q) - (\beta_{xz} \tau) \frac{\partial u}{\partial y} + u \frac{\partial}{\partial x} (\beta_{yz} P) + \rho C_D u^3 D(y) / 2Lx + \pi \mu c (Nu) (T_R - T) / PrLL$$

Where: $\beta_{xz} = \beta_{yz} = (1 - \frac{\pi D^2(y)}{4LL})$, the blockage factor
 $C_D = C_D(Re(y))$, the roughness element drag coefficient
 $Nu = Nu(Re(y))$, the roughness element Nusselt number
 $Re(y) = u(y)D(y)/\nu$, the local Reynolds number
 $D(y) =$ roughness element diameter
 $L, l =$ roughness element spacing in longitudinal and transverse directions

Figure 2. 2-D Compressible Turbulent Boundary Layer Equations Including Roughness Effects

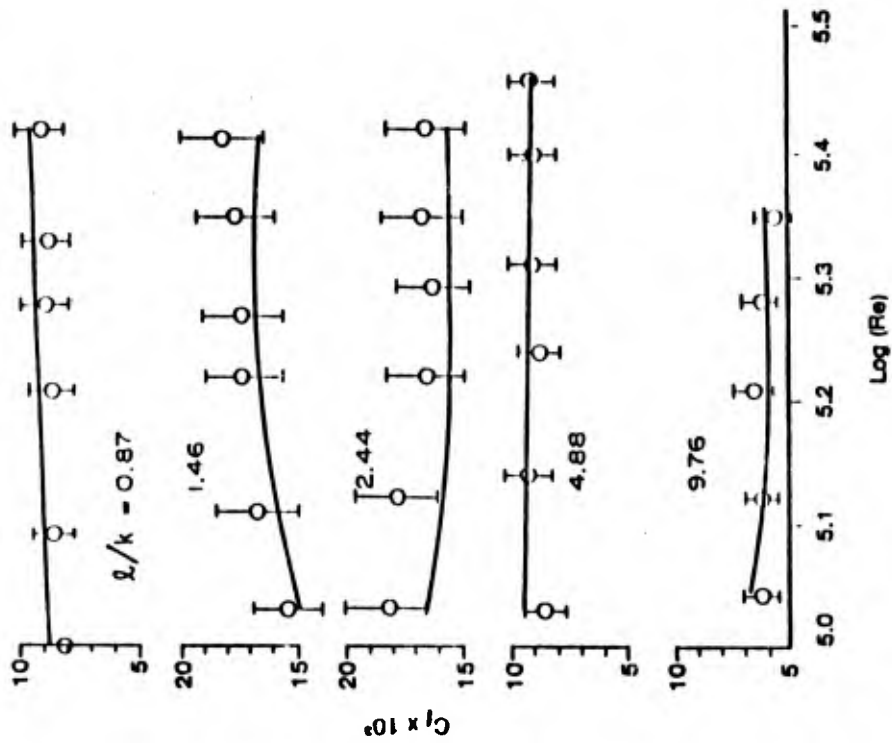


Figure 3. Comparison of Calculations with the Corrected Skin Friction Data of Schlichting for Spheres (Calibration Data)

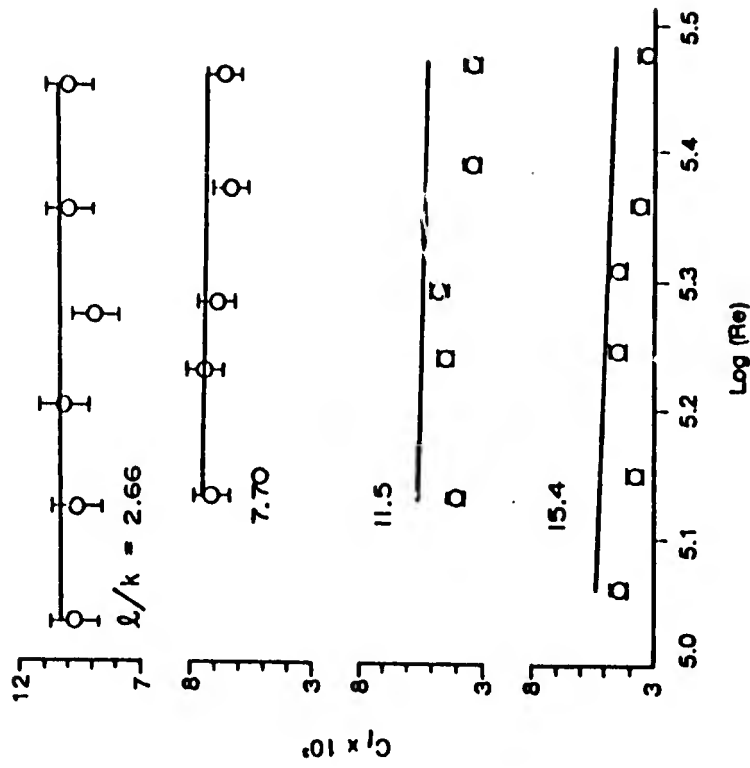


Figure 4. Comparison of Calculations with the Corrected Skin Friction Data of Schlichting for Spherical Segments (Calibration Data)

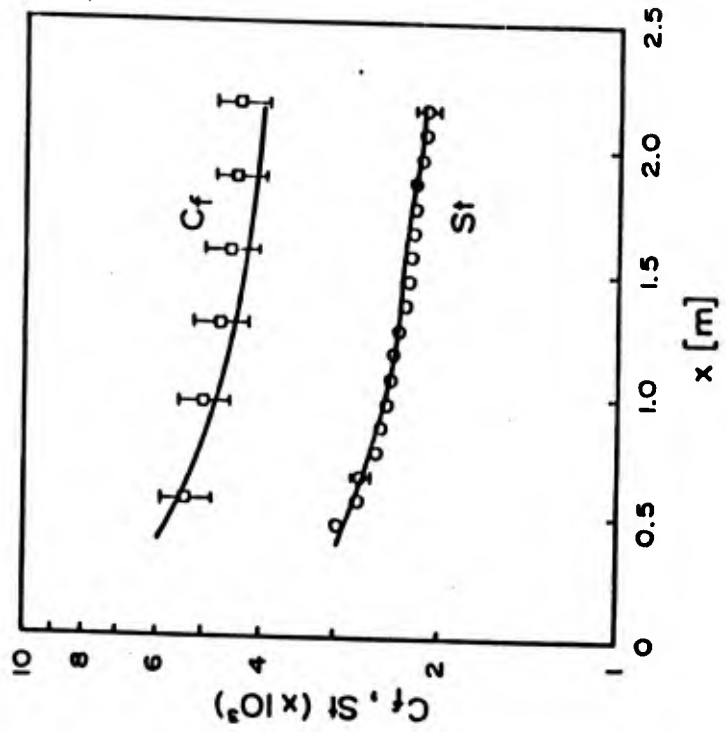


Figure 6. Comparison of Calculations with the Flat Plate Stanton Number (Calibration) Data of Pimenta and Comparison of Predictions with Skin Friction Data. $u_{\infty} = 27$ m/sec.

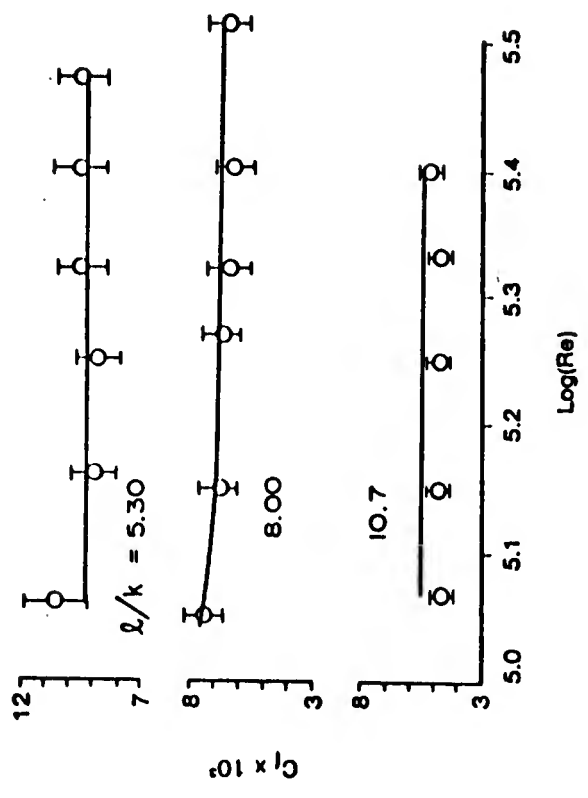


Figure 5. Comparison of Calculations with the Corrected Skin Friction Data of Schlichting for Cones (Calibration Data)

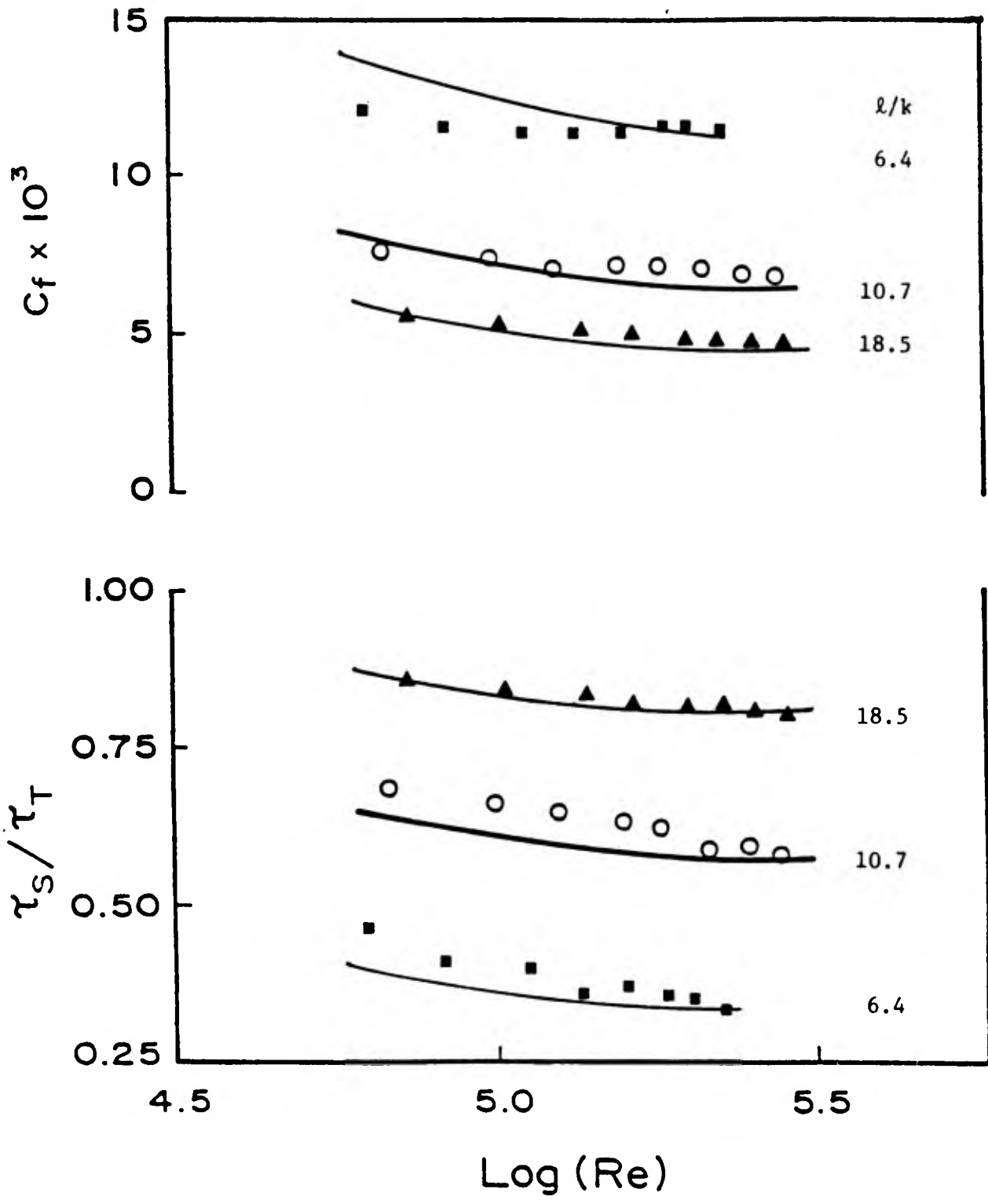


Figure 7. Comparison of Discrete Element Model Predictions with the Data of Chen

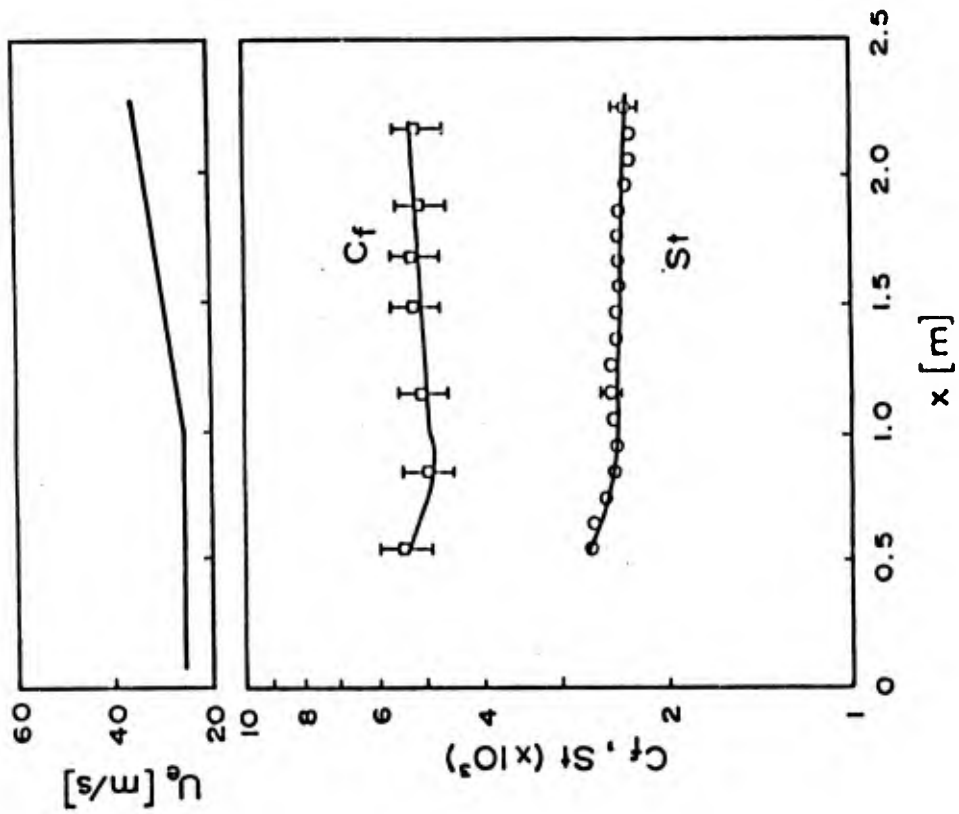


Figure 8. Comparison of Predictions with Data of Coleman for Turbulent Boundary Layer on a Constant Temperature Flat Plate with Favorable Pressure Gradient Imposed

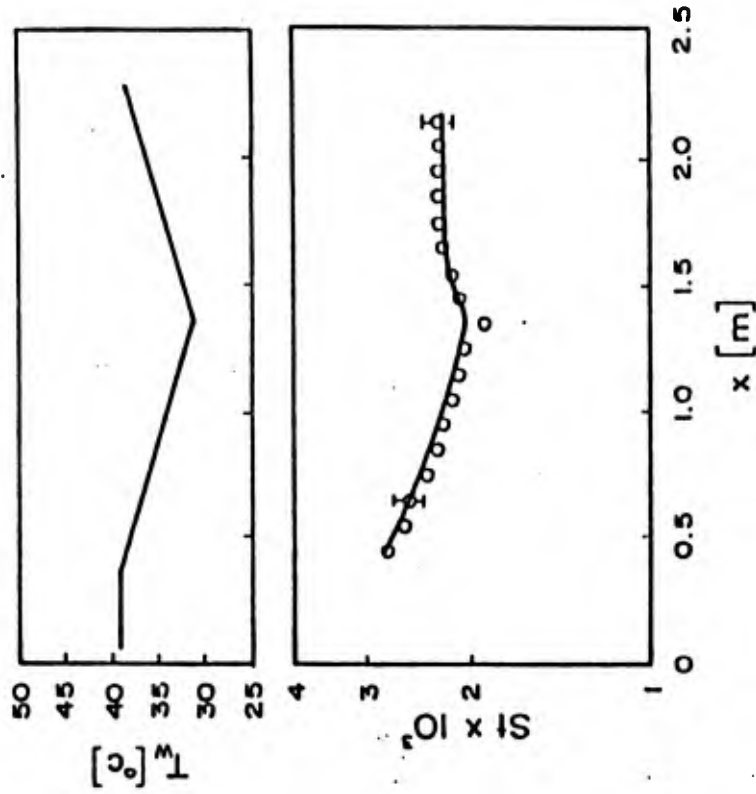


Figure 9. Comparison of Calculations with the Data of Coleman; Bi-linear Wall Temperature Distribution